Bioimaging

DOI: 10.1002/anie.201109089

Carbon-Dot-Based Dual-Emission Nanohybrid Produces a Ratiometric Fluorescent Sensor for In Vivo Imaging of Cellular Copper Ions**

*Anwei Zhu, Qiang Qu, Xiangling Shao, Biao Kong, and Yang Tian**

The integration of highly specific recognition elements, such as organic molecules or biomolecules, into inorganic nanomaterials of unique electronic and optical characteristics, such as gold nanostructures, carbon nanotubes, or semiconductor nanoparticles, has made possible many new strategies for bioanalysis and bioimaging techniques.[1] Carbon quantum dots (CQDs) have attracted tremendous attention because of their interesting properties, such as non-blinking, water solubility, and nontoxicity according to currently available cytotoxic and in vivo toxic evaluation results.[2] However, exploration of CQDs as fluorescent chemosensors to monitor and image biological processes still remains in the early stage.[3] Herein, we first design a ratiometric CQD-based fluorescent probe for intracellular sensing and imaging of Cu^{2+} ions with high selectivity, sensitivity, and photostability.

Since intracellular Cu^{2+} ions play a critical role in physiological and pathological events,[4] new methods for monitoring Cu^{2+} ions in living cells can help to understand their complex contributions to healthy and disease states. Biological imaging with optically sensitive Cu^{2+} indicators provides an attractive approach to achieve this goal. Recently, several efficient fluorescent sensors for Cu^{2+}-selective detection were reported.[5] However, the development of a ratiometric fluorescence method for intracellular measurement of Cu^{2+} ions is still limited by the design of new dual-emission organic fluorophores which are specific and sensitive to Cu^{2+} ions,[6a] although ratiometric sensors have attracted significant attention as an alternative to first-generation intensity probes because of their sensitivity and built-in correction for environmental effects.[6]

Herein, we first integrated an organic molecule specific for Cu^{2+} ions, *N*-(2-aminoethyl)-*N*,*N*,*N*′tris(pyridin-2-ylmethyl)ethane-1,2-diamine (AE-TPEA), into a hybrid system composed of carbon and CdSe/ZnS quantum dots (QDs) and thus developed a selective and sensitive ratiometric strategy for intracellular sensing and imaging of Cu^{2+} ions. As illustrated in Scheme 1, the CQDs emitting blue fluorescence are hybridized with CdSe/ZnS QDs emitting red fluorescence as dual-emission fluorophore (CdSe@C nanohybrid), in which CdSe/ZnS QDs embedded in silica shells ($CdSe@SiO_2$) are inert to Cu^{2+} ions and only serve as reference signals for providing built-in correction to avoid environmental effects. Meanwhile, AE-TPEA acting as a specific receptor for Cu^{2+} ions is synthesized and conjugated with the responsive CdSe@C nanohybrid to form inorganic–organic CdSe@C-TPEA probes. The hybrided probe shows dual emission bands centered at 485 and 644 nm, respectively, under single wavelength excitation of 400 nm. The blue CQDs functionalized with AE-TPEA ($\lambda_{em} = 485$ nm) can selectively recognize Cu^{2+} ions, leading to blue fluorescence quenching, whereas the fluorescence of red $CdSe@SiO_2$ particles ($\lambda_{em} = 644$ nm) stays constant. Consequently, variation of the two fluorescence intensities (I_{485}/I_{644}) displays the continuous color changes upon addition of Cu^{2+} ions, which can be easily observed by the naked eyes under a UV lamp, resulting in a ratiometric fluorescent sensor for Cu^{2+} ions. The specific nanohybrid can monitor Cu^{2+} ions in a concentration range from 5×10^{-6}–2×10^{-4} M in a physiological pH environment. The ratiometric fluorescent probe also shows high selectivity toward Cu^{2+} ions over competing metal ions at cellular concentrations. Notably, compared with dual-emission organic fluorophores, the CdSe@C nanocomposites show good water dispersibility and high stability against light illumination, pH changes, and exposure to air, as well as low cytotoxicity, because CdSe/ZnS QDs with serious health and environmental concerns are embedded in silica shells and further surrounded with low-toxic CQDs. As expected, real-time imaging and biosensing of cellular Cu^{2+} ions was successfully achieved in living cells. To the best of our knowledge, it is the first time that a CQD-based ratiometric

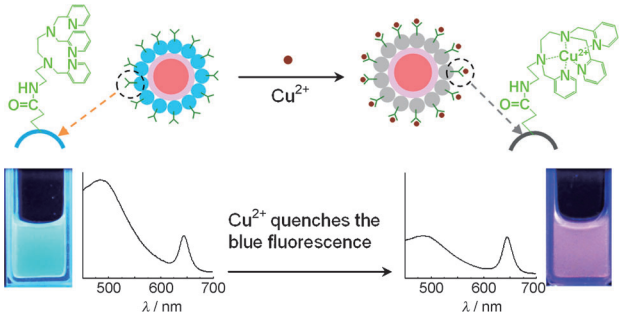

Scheme 1. Dual-emission fluorescent sensing of Cu^{2+} ions based on a CdSe@C-TPEA nanohybrid.

[*] A. Zhu,[+] Q. Qu,[+] X. Shao, B. Kong, Prof. Dr. Y. Tian
Department of Chemistry, Tongji University
Siping Road 1239, Shanghai 200092 (P. R. China)
E-mail: yangtian@mail.tongji.edu.cn

[+] These authors contributed equally to this work.

[**] This work was financially supported by the National Natural Science Foundation of China (NSFC, grant numbers 20975075 and 21175098), and the Fundamental Research Funds for the Central Universities.

Supporting information for this article is available on the WWW under http://dx.doi.org/10.1002/anie.201109089.

© 2012 Wiley-VCH Verlag GmbH & Co. KGaA, Weinheim

fluorescence probe has been successfully used for biological sensing and imaging.

As a starting point of our study, CQDs were synthesized by an electrochemical method.[7] A typical TEM image (Figure 1a) shows that the as-prepared CQDs are monodispersed with an average size of around 5 nm. From the cross-sectional view of the AFM image (see Figure S1 in the Supporting Information), the average thickness of CQDs is around 4 nm. The UV/Vis absorption peaks of the CQDs at 250–300 nm represent a typical absorption of an aromatic π system (see Figure S2 in the Supporting Information). The fluorescence intensity of the CQDs is strong enough to be easily seen with the naked eye. The bare CQDs show a strong emission at 491 nm upon excitation at 400 nm (see Figure S2 in the Supporting Information). Using rhodamine B as a standard, the fluorescence quantum yield (QY) of CQDs was calculated to be around 10%. The infrared (IR) spectrum of the CQDs is given in Figure 1b. The bands at around 2974 and 1602 cm^{-1} correspond to the C=C stretching modes of polycyclic aromatic hydrocarbons. The band at around 1680 cm^{-1} indicates the existence of carbonyl (C=O) groups, whereas the bands at around 1727 and around 1096 cm^{-1} are due to carboxylic groups. The band at around 3425 cm^{-1} corresponds to the OH stretching mode. These data demonstrate that the as-prepared CQDs are surrounded by -COOH and/or -OH groups.

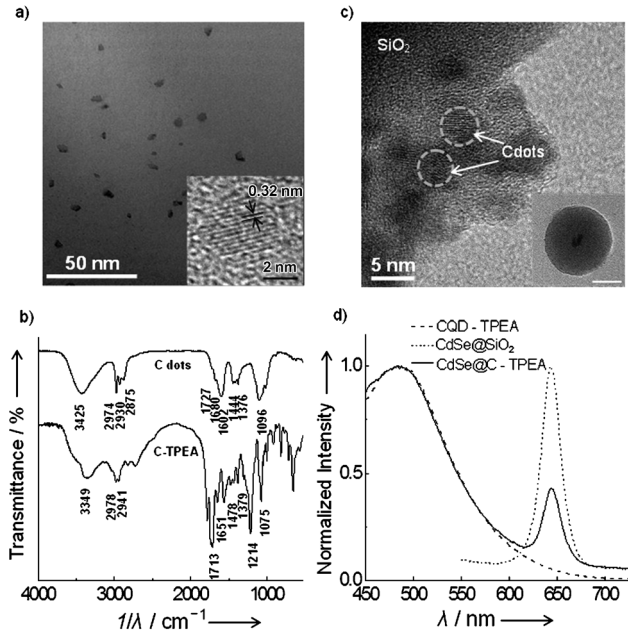

Figure 1. a) TEM image of the CQDs and HRTEM image of typical CQDs (inset). b) FT-IR spectra of as-prepared CQDs and CQD-TPEA. c) HRTEM image of a portion of a typical CdSe @C-TPEA particle. Inset: TEM image of a typical CdSe@SiO_2 particle. d) Normalized fluorescence emission spectra of CQD-TPEA (dashed line), CdSe@-SiO_2 (short dashed line), and the CdSe@C-TPEA hybrid (solid line).

On the other hand, by the modified reverse microemulsion method,[8] CdSe/ZnS QDs were first coated with inert silica and then modified with amino groups to improve their chemical and photochemical stabilities, as well as water solubility and labeling ability. A typical TEM image of core–shell-structured CdSe@SiO_2 particles is presented in the inset of Figure 1c and Figure S4 (see the Supporting Information). Although the fluorescent intensity of CdSe/ZnS QDs partly decreased after being surrounded by SiO_2 shells (see Figure S3 in the Supporting Information), the composite particles that were finally obtained still showed strong fluorescence with emission band centered at 644 nm (see Figure S4 in the Supporting Information). By taking advantage of the possible electrostatic interactions between the amine group on the SiO_2 particles and the carboxy residues of the CQDs, the obtained CdSe@C nanocomposites (Figure 1c) show well-resolved dual emission (Figure 1d green curve).

To further confer the water-soluble CdSe@C nanohybrid selectivity for the model target Cu^{2+} ions, we designed and synthesized an organic molecule containing an amine group (AE-TPEA) by substitution of TPEA with *N*-(2-bromoethyl)phthalimide in acetonitrile followed by deprotection of the product with hydrazine hydrate. The structure of AE-TPEA was confirmed by ^1H NMR, ^{13}C NMR spectroscopies, and HR-MS (see Figures S5–S7 in the Supporting Information). Then, AE-TPEA molecules were conjugated with the CdSe@C nanohybrid by using 1-ethyl-3-(3-dimethylaminopropyl) carbodiimide hydrochloride (EDC) and *N*-hydroxysuccinimide (NHS) as catalysts. As shown in Figure 1d (black curve), the CQD-TPEA shows strong emission at 485 nm upon excitation at 400 nm, a little blue-shifted (6 nm) compared with that of bare CQDs (Figure S2 in the Supporting Information). The ability of AE-TPEA to attach onto the surface of the CQDs was also confirmed by IR spectroscopy. As shown in Figure 1b, the band at around 3349 cm^{-1} corresponds to the stretching vibration of N–H groups. The bands located at around 1478 cm^{-1} and 1651 cm^{-1} are ascribed to the bending vibration of the N–H group and the stretching vibration of C=O groups, respectively, indicating the successful formation of an amide group between CQDs and AE-TPEA.

The response of the dual-emission fluorescent probe towards Cu^{2+} ions ($CuCl_2$) was then carried out to prove the working principle, as demonstrated in Figure 2. The ratiometric probe shows two emission bands centered at 485 and 644 nm, which are ascribe to the emission from blue CQD-TPEA on the surface and red CdSe/ZnS QDs embedded in silica nanoparticles, respectively, under single-wavelength excitation at 400 nm. Upon addition of Cu^{2+} ions, as shown in Figure 2a, the intensity of blue emission from the reactive CQDs shows continuous quenching, whereas that of red emission from the encapsulated CdSe/ZnS QDs still remains constant. The changes in the intensities of the two emission peaks result in continuous fluorescence color changes as demonstrated in Figure 2b. Clearly, even a slight decrease of the blue emission intensity can be distinguished from the original background with the naked eyes. The advantages of the ratiometric fluorescence for visual detection can be confirmed by comparison with a single fluorescence quenching experiment, in which only a CQD-TPEA probe was employed for the detection of Cu^{2+} ions, as shown in Figure 2c and d. Unlike the ratiometric probe, fluorescence

 © 2012 Wiley-VCH Verlag GmbH & Co. KGaA, Weinheim

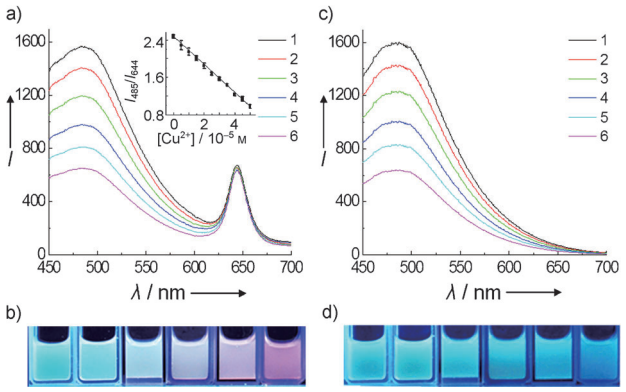

Figure 2. Fluorescence spectra (λ_{ex} = 400 nm) of a) the CdSe@C-TPEA ratiometric probe and c) the CQD-TPEA, upon the exposure to different amounts of $CuCl_2$. b, d) Comparison between the fluorescence colors of the ratiometric probe solutions (b) and the CQD-TPEA solutions (d) after exposure to $CuCl_2$. The concentrations of $CuCl_2$ from left to right are 0, 10, 20, 30, 40, and 50 μM, respectively. The inset of (a) shows the plot of I_{486}/I_{644} as a function of the Cu^{2+} concentration obtained with 0.02 mg mL^{-1} CdSe@C-TPEA (pH 7.4).

images of the pure CQDs are hard to distinguish among the other images by the naked eye (Figure 2d). The results indicate that the ratiometric fluorescent probe is more sensitive and reliable for visual detection of Cu^{2+} ions than a single fluorescence quenching probe, although the intensity of the blue channel decreases at almost the same level. As shown in the inset of Figure 2a, the intensity ratio of the two emission wavelengths (I_{485}/I_{644}) gradually decreases with increasing concentration of Cu^{2+} ions and the signal ratio shows good linearity with the Cu^{2+} concentration in the range of around 10^{-6}–10^{-4} M. The linear range meets the requirement for in vivo imaging and sensing of Cu^{2+} ions, because the concentration of intracellular Cu^{2+} ions is well reported to be around 10^{-5} M.[10] The detection limit was calculated to be around 1 μM (based on a signal-to-noise ratio of S/N = 3). In addition, the reaction between TPEA and Cu^{2+} ions was complete within 1 min (see Figure S8 in the Supporting Information). This observation suggests that the inorganic–organic nanohybrid with quick response can be employed as fluorescent probe for real-time tracking of Cu^{2+} ions in the biological system.

In addition, no significant changes (< 5%) of the fluorescent responses at 485 and 644 nm are observed under 400 nm excitation up to around 2 h in 10 mM phosphate buffered saline (PBS) solution (pH 7.0, see Figure S9 in the Supporting Information), indicating the long-term photostability of the CdSe@C-TPEA probe. Furthermore, the fluorescent responses of the hybrid are also observed to be stable in solution with a broad pH range (see Figure S10 in the Supporting Information). These observations indicate that superior to organic fluorophores, the CQD-based fluorescent sensors show excellent stability against light illumination, pH variation, and exposure to air.

The complexity of intracellular system presents a great challenge to the analytical methods for metal ion detection not only in sensitivity but more importantly in selectivity. Then, the selectivity experiments were carried out by monitoring the intensity ratio (I_{485}/I_{644}) of the probe in the presence of other metal ions that may coexist in the living cells. First, various metal ions such as abundant cellular cations (Na^+, K^+, Ca^{2+}, Mg^{2+}) and trace metal cations in organisms (Mn^{2+}, Fe^{2+}, Co^{2+}, Ni^{2+}, Zn^{2+}, Cu^+) were tested. Remarkably, as shown in Figure 3a, no obvious changes of the signal were observed for the other metal ions, compared with that obtained for Cu^{2+} ions. Furthermore, these potential metal ion interferences showed negligible effects on the signal for Cu^{2+} sensing. Although the clear mechanism for good selectivity against other metal ions was still unknown at the present stage, the possible reasons were discussed (see Figure S11 in the Supporting Information).

Taking into account that amino acids in the biological system are capable of interacting with many metal cations, several typical amino acids were also examined as potential interferences. As shown in Figure 3b, little effect on the

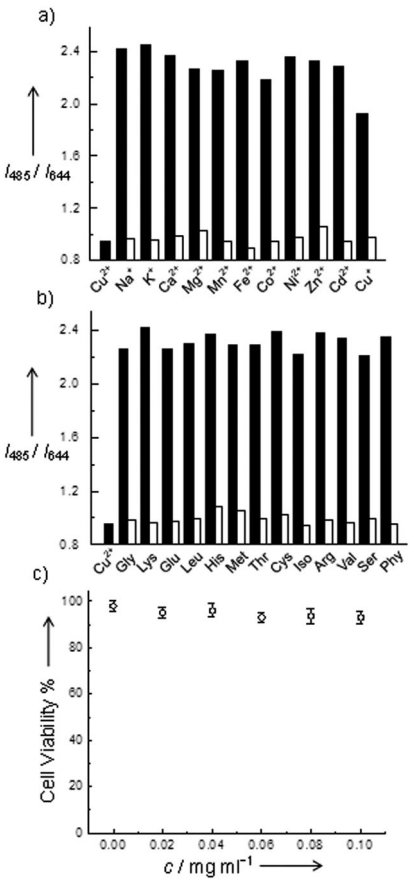

Figure 3. a) Fluorescence responses of CdSe@C-TPEA towards various metal ions. The black bars represent the addition of an excess of metal ions (1 mM for Na^+, K^+, Ca^{2+}, and Mg^{2+}; 50 μM for other cations) to a 0.02 mg mL^{-1} solution of CdSe@C-TPEA (pH 7.4). The white bars represent the subsequent addition of 50 μM Cu^{2+} ions to the solution. b) Fluorescence responses of CdSe@C-TPEA toward various amino acids. The black bars represent the addition of 100 μM amino acid to a 0.02 mg mL^{-1} solution of CdSe@C-TPEA (pH 7.4). The white bars represent the subsequent addition of 50 μM Cu^{2+} ions to the solution. The excitation wavelength was set to 400 nm. c) Cell viability values (%) estimated by MTT proliferation tests versus incubation concentrations of CdSe@C-TPEA (0, 0.02, 0.04, 0.06, 0.08, 0.1 mg mL^{-1}) at 310 K for 24 h.

 © 2012 Wiley-VCH Verlag GmbH & Co. KGaA, Weinheim

intensity ratio of the probes was observed after their exposure to a concentration of amino acids which was the same as that of the Cu^{2+} ions. On the other hand, the effect of all these amino acids on the signal of the Cu^{2+} ions was also investigated in detail. Negligible signal changes were observed when all the above compounds were added to the solution in the presence of Cu^{2+} ions. All the results indicate that the present CdSe@C-TPEA nanohybrids show a high selectivity for Cu^{2+} biosensing against other metal ions and amino acids.

For further biological applications, MTT (MTT = 3-(4,5-dimethylthiazol-2-yl)-2,5-diphenyltetrazolium bromide) assays were carried out to evaluate the cytotoxicity of the inorganic–organic probes to Hela cells. As expected, the viability of the Hela cells declined only by $<5\%$ upon addition of the fluorescent probes at up to 0.10 mg mL^{-1} (Figure 3c). Thus, the as-prepared CdSe@C-TPEA probe can be considered to be low toxic and biocompatible for detection of Cu^{2+} ions in living cells.

Although the bulk of the intracellular copper is believed to be present in its monovalent oxidation state, the subcellular microenvironment may support the Cu^{2+} ions. The advantages of the carbon-dot-based dual-emission nanohybrid system also incited us to access its performance in monitoring the dynamic changes in the Cu^{2+} concentration during transient formation in a deleterious redox cycling process. To this end, Hela cells were first incubated with the probe and phorbol-12,13-dibutyrate (PDBu, a compound known to increase the endocytic activity) in PBS (pH 7.4) for 2 h at 37 °C.[10] After the uptake, the particles were monitored by confocal microscopy and found to reside in various intracellular compartments (Figure 4a,b). Meanwhile, the fluorescence scan in Hela cells treated with the fluorescent probe confirmed that the nanohybrid had a good cell-permeability and maintained its dual-emission characteristic in a cellular environment (see Figure S12 in the Supporting Information). Then, the intracellular Cu^{2+} imaging ability of CdSe@C-TPEA was tested. In this context, pyrrolidine dithiocarbamate (PDTC) was employed to increase the intracellular level of the Cu^{2+} ions.[11] After the exogenous Cu source treatment, the fluorescence emission color of the probe turned from green-yellow (Figure 4b) to red (Figure 4c), which agreed well with a change of the fluorescence spectrum observed in Hela cells (see Figure S12 in the Supporting Information). This change is summarized in the bar graph of Figure 4d and was more clearly observed from the separated channels. As depicted in Figure 4e–h, the green fluorescence image from the CQDs became dimmer after addition of the Cu source and incubation for 2 h, whereas the red reference channel showed almost no change. These initial experiments on living cells show the great potential of carbon-dot-based dual-emission nanohybrid systems for fundamental biology research.

In summary, by preparing dual-emission CdSe@C QDs as fluorophores and designing amino-TPEA as the receptor, which can recognize Cu^{2+} with high specificity, we have developed a selective and sensitive strategy for the ratiometric fluorescent detection of Cu^{2+} ions with long-term stability. The inorganic–organic fluorescent probe showed good cell permeability and low cytotoxicity, and thus can be successfully applied for imaging and biosensing of Cu^{2+} ions in living cells. This work provides a method for designing CQD-based ratiometric fluorescent assays with high specificity and sensitivity for in vivo imaging and biosensing of metal ions and biological molecules. A sensitive and reliable approach was established for monitoring intracellular metal ions and other species in living cells, which may be related to physiological and pathological events.

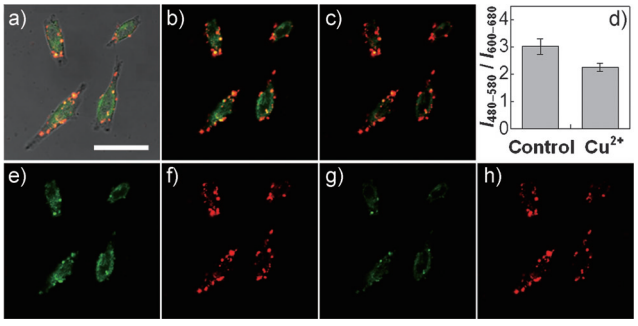

Figure 4. a) The overlay of bright-field and fluorescence images of Hela cells incubated with 0.05 mg mL^{-1} CdSe@C-TPEA and 0.1 μM PDBu in PBS (pH 7.4) for 2 h at 310 K and 5% CO_2. Panels (b) and (c) are the confocal fluorescence images of Hela cells before (b) and after (c) the exogenous Cu source treatment (addition of 100 μM $CuCl_2$ and 100 μM PDTC to the petri dish). d) A bar graph showing the integrated intensity from 480–580 nm over the integrated fluorescence intensity from 600–680 nm. Values are the mean ratio generated from the intensity from three randomly selected fields in both channels. The error bars represent standard error measurement (s.e.m). Panels (e) and (g) are the confocal fluorescence images obtained from 480–580 nm before and after the exogenous Cu source treatment, whereas panels (f) and (h) are the confocal fluorescence images obtained from 600–680 nm. Scale bar: 25 μm.

Received: December 23, 2011
Revised: February 13, 2012
Published online: March 8, 2012

Keywords: analytical methods · carbon · copper · fluorescence spectroscopy · imaging agents

[1] a) M. Bruchez, Jr., M. Moronne, P. Gin, S. Weiss, A. P. Alivisatos, *Science* **1998**, *281*, 2013–2016; b) Z. Chen, H. Chen, H. Hu, M. Yu, F. Li, Q. Zhang, Z. Zhou, T. Yi, C. Huang, *J. Am. Chem. Soc.* **2008**, *130*, 3023–3029; c) Y. Lin, S. Taylor, H. Li, K. A. S. Fernando, L. Qu, W. Wang, L. Gu, B. Zhou, Y. P. Sun, *J. Mater. Chem.* **2004**, *14*, 527–541; d) B. Kong, A. Zhu, Y. Luo, Y. Tian, *Angew. Chem.* **2011**, *123*, 1877–1880; *Angew. Chem. Int. Ed.* **2011**, *50*, 1837–1840; e) A. Zhu, Y. Luo, Y. Tian, *Chem. Commun.* **2009**, 6448–6450; f) A. Zhu, Y. Luo, Y. Tian, *Anal. Chem.* **2009**, *81*, 7243–7247.

[2] a) S. T. Yang, L. Cao, P. G. Luo, F. Lu, X. Wang, H. Wang, M. J. Meziani, Y. Liu, G. Qi, Y. P. Sun, *J. Am. Chem. Soc.* **2009**, *131*, 11308–11309; b) S. Yang, X. Wang, H. Wang, F. Lu, P. G. Luo, L. Cao, M. J. Meziani, J. Liu, Y. Liu, M. Chen, Y. Huang, Y. P. Sun, *J. Phys. Chem. C* **2009**, *113*, 18110–18114; c) S. N. Baker, G. A. Baker, *Angew. Chem.* **2010**, *122*, 6876–6896; *Angew. Chem. Int. Ed.* **2010**, *49*, 6726–6744.

© 2012 Wiley-VCH Verlag GmbH & Co. KGaA, Weinheim

[3] H. Gonçalves, P. A. S. Jorge, J. R. A. Fernandes, J. C. G. Esteves da Silva, *Sens. Actuators B* **2010**, *145*, 702 – 707.
[4] a) M. C. Linder, M. Hazegh-Azam, *Am. J. Clin. Nutr.* **1996**, *63*, 797S – 811S; b) R. Uauy, M. Olivares, M. Gonzalez, *Am. J. Clin. Nutr.* **1998**, *67*, 952S – 959S; c) K. J. Barnham, C. L. Masters, A. I. Bush, *Nat. Rev. Drug Discovery* **2004**, *3*, 205 – 214.
[5] a) J. Liu, Y. Lu, *J. Am. Chem. Soc.* **2007**, *129*, 9838 – 9839; b) W. Lin, L. Yuan, W. Tan, J. Feng, L. Long, *Chem. Eur. J.* **2009**, *15*, 1030 – 1035; c) Y. Zhao, X. B. Zhang, Z. X. Han, L. Qiao, C. Y. Li, L. X. Jian, G. L. Shen, R. Q. Yu, *Anal. Chem.* **2009**, *81*, 7022 – 7030; d) K. C. Ko, J. S. Wu, H. J. Kim, P. S. Kwon, J. W. Kim, R. A. Bartsch, J. Y. Lee, J. S. Kim, *Chem. Commun.* **2011**, *47*, 3165 – 3167.
[6] a) D. W. Domaille, L. Zeng, C. J. Chang, *J. Am. Chem. Soc.* **2010**, *132*, 1194 – 1195; b) M. Royzen, Z. Dai, J. W. Canary, *J. Am. Chem. Soc.* **2005**, *127*, 1612 – 1613; c) K. Komatsu, Y. Urano, H. Kojima, T. Nagano, *J. Am. Chem. Soc.* **2007**, *129*, 13447 – 13454; d) C. Wu, B. Bull, K. Christensen, J. McNeill, *Angew. Chem.* **2009**, *121*, 2779 – 2783; *Angew. Chem. Int. Ed.* **2009**, *48*, 2741 – 2745; e) Z. Xu, J. Yoon, D. R. Spring, *Chem. Commun.* **2010**, *46*, 2563 – 2565; f) K. Zhang, H. Zhou, Q. Mei, S. Wang, G. Guan, R. Liu, J. Zhang, Z. Zhang, *J. Am. Chem. Soc.* **2011**, *133*, 8424 – 8427; g) H. Yu, Y. Xiao, H. Guo, X. Qian, *Chem. Eur. J.* **2011**, *17*, 3179 – 3191; h) F. Ye, C. Wu, Y. Jin, Y. H. Chan, X. Zhang, D. T. Chiu, *J. Am. Chem. Soc.* **2011**, *133*, 8146 – 8149.
[7] H. Li, X. He, Z. Kang, H. Huang, Y. Liu, J. Liu, S. Lian, C. H. A. Tsang, X. Yang, S. T. Lee, *Angew. Chem.* **2010**, *122*, 4532 – 4536; *Angew. Chem. Int. Ed.* **2010**, *49*, 4430 – 4434.
[8] Y. Yang, M. Gao, *Adv. Mater.* **2005**, *17*, 2354 – 2357.
[9] M. Yu, M. Shi, Z. Chen, F. Li, X. Li, Y. Gao, J. Xu, H. Yang, Z. Zhou, T. Yi, C. Huang, *Chem. Eur. J.* **2008**, *14*, 6892 – 6900.
[10] a) C. Ra, K. Furuichi, J. Riviera, J. Mullins, C. Isersky, K. White, *Eur. J. Immunol.* **1989**, *19*, 1771 – 1777; b) A. Alcover, B. Alarcon, *Crit. Rev. Immunol.* **2000**, *20*, 325 – 346.
[11] G. W. Verhaegh, M. Richard, P. Hainaut, *Mol. Cell. Biol.* **1997**, *17*, 5699 – 5706.

 © 2012 Wiley-VCH Verlag GmbH & Co. KGaA, Weinheim